Observation of temperature independent heterogeneous electron transfer reactions in the inverted Marcus region

Jacques E. Moser and Michael Grätzel

Institut de Chimie Physique, Ecole Polytechnique Fédérale, CH-1015 Lausanne, Switzerland

Measurements have been performed of the temperature dependence of highly exoergic interfacial electron transfer processes from the conduction band of nanocrystalline titanium dioxide to the cation radicals of three different sensitizers, i.e alizarin, a merocyanine and a coumarin dye. Although these reactions fall deep into the inverted Marcus region, they show practically no activation energy. The results are interpreted in terms of a quantum mechanical model for non-adiabatic electron transfer including the treatment of high frequency molecular vibrations of the adsorbed sensitizer. This analysis provides apart from the electronic matrix coupling elements separate values for the internal and solvent reorganization energies. The behavior of the alizarin/ TiO_2 chelate is unusual in as much as the solvent reorganization does not appear to contribute significantly to the interfacial redox process.

1. Introduction

Heterogeneous electron transfer reactions play a vital role in a great variety of important phenomena associated with the operation of electronic, electrochemical, photo-electrochemical and other devices [1]. The rate constant for charge transfer processes across the solid-electrolyte interface is usually described in terms of the Tafel equation [2]. For a cathodic one-electron process:

$$k = k^0 \exp[-\alpha F(E - E^0)/RT] . \quad (1)$$

Here α is the transfer coefficient, E is the electrode potential, F is Faraday's constant, and k^0 is the rate constant at the reference potential E^0. Alternatively, the rate constant may be expressed by the classical Marcus relation for non-adiabatic electron transfer [3]:

$$k = \nu_0 \kappa \exp[-(\Delta_r G^0 + \Lambda)^2/4\Lambda RT] , \quad (2)$$

where ν_0 is a frequency factor, κ is the electronic coefficient, $\Delta_r G^0$ is the standard free energy of the reaction and Λ is the total reorganization energy. The Tafel equation predicts that the reaction rate constant should vary exponentially with $1/T$. Similarly, from the classical Marcus expression one expects an expo-

nential temperature dependence both in the normal ($-\Delta_r G^0 < \Lambda$) and inverted ($-\Delta_r G^0 > \Lambda$) region. Only for the case where $-\Delta_r G^0$ equals Λ should the electron transfer process become activationless.

While the inverted Marcus regions has attracted many investigators, these studies have focused on the verification of the decrease in the electron transfer rate with increasing driving force [4]. Only two recent investigations address the question of temperature effects on the rate coefficient in the inverted region [5,6]. In both cases authors studied an intramolecular charge transfer process. Activationless behavior was observed which was ascribed to vibronic coupling effects.

The present investigation scrutinizes for the first time the effect of temperature on a heterogeneous redox reaction occurring in the inverted Marcus region. Due to their rapid nature and the limited temperature range accessible to liquid electrolytes, such interfacial electron transfer processes are difficult to follow by conventional electrochemical techniques. The advent of nanocrystalline semiconductors forming transparent colloidal solutions has opened up the way to monitor this type of reactions directly by time resolved laser spectroscopy [7,8]. Here we report on investigations with dispersions of nanocrystalline ti-

tanium dioxide particles whose surface has been derivatized with a monolayer of charge transfer sensitizer. The dynamics of the reverse electron transfer from the conduction band of the semiconductor to the sensitizer radical cation following light induced charge injection have been investigated and are shown to be surprisingly insensitive to temperature changes extending over more than two hundred degrees.

2. Experimental

2.1. Materials

Alizarin supplied by Fluka was recrystallized three times from hot ethanol–water solutions. The carboxylated thiazole rhodanine merocyanine, Mc2, was purchased from Riedel-de-Haën and further purified by recrystallization in acidified water. Coumarin-343 (laser grade) was used as obtained from Kodak. The molecular structures of these charge transfer sensitizers are shown in scheme 1. All three dyes are endowed with suitable interlocking groups whose role is to graft the dye to the semiconductor surface via chelation of surface titanium ions. Although absorption spectra of the merocyanine and coumarin-343 are only slightly affected by adsorption on the oxide surface, a large 70 nm red shift and an increase of the
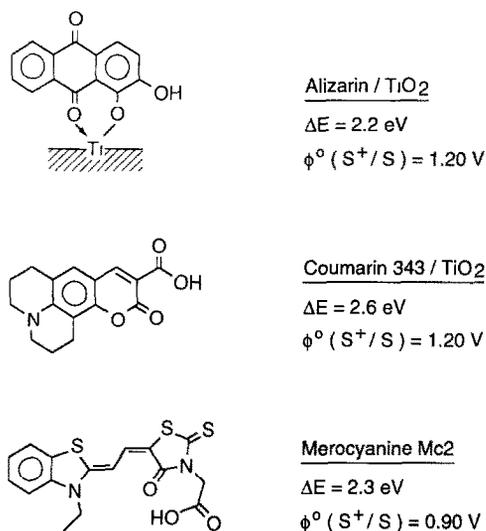
extinction coefficient from 3.6×10^3 mol^{-1} ℓ cm^{-1} to more than 10^4 mol^{-1} ℓ cm^{-1} is observed for alizarin upon complexation of the titanium dioxide surface. In the latter case, a surface alizarin–Ti(IV) charge transfer complex has therefore to be considered as the active chromophore. For all three sensitizers, photoinduced electron injection into the conduction band of TiO_2 occurs with close to unit quantum efficiency. The redox potentials of the sensitizers were determined in ethanol/methanol 5:1 (v/v) mixture by cyclic voltammetry. 4 μm thick nanocrystalline TiO_2 film deposited onto a conductive glass support [9] and surface derivatized with the respective dye was used as the working electrode. Values for these potentials (versus NHE) as well as those for the 0–0 electronic transition energies are indicated in scheme 1.

Colloidal TiO_2 solutions were prepared in ethanol by a previously described procedure [10]. Methanol was subsequently added to decrease the glass transition temperature to ≈ 100 K. The mean radius of the anatase nanocrystals was between 5 and 10 nm.

All other chemicals were at least reagent grade and were used as supplied by the vendor.

2.2. Methods

Time resolved absorption measurements were carried out using 8 ns, 530 nm Nd:YAG laser pulses as the excitation source for alizarin and Mc2 systems on a flash photolysis set up. 10 ns, 450 nm pulses from a dye laser pumped by a frequency-doubled ruby laser were used to excite coumarin-343. The optical signal was detected using a Hamamatsu R928 PM tube. Data acquisition and analysis were performed by a Tektronix DSA 602A digital signal analyzer connected to an Apple Macintosh computer. For temperature control, the colloidal solution contained in a square quartz cell was mounted in a Oxford Instruments DN1704 nitrogen bath cryostat equipped with an ITC-4 controller. The temperature domain studied was between -200°C and 30°C. All solutions were carefully degassed by repeated freeze–pump–thaw cycles prior to use.

Alizarin / TiO_2

$\Delta E = 2.2$ eV

$\phi^{\circ}(S^+/S) = 1.20$ V

Coumarin 343 / TiO_2

$\Delta E = 2.6$ eV

$\phi^{\circ}(S^+/S) = 1.20$ V

Merocyanine Mc2

$\Delta E = 2.3$ eV

$\phi^{\circ}(S^+/S) = 0.90$ V

Scheme 1

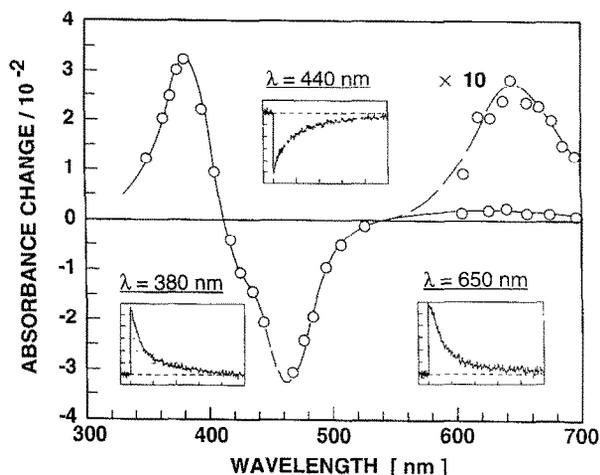## 3. Results

Figs. 1–3 show transient absorption spectra ob-

Fig. 1. Transient absorption spectrum observed upon pulsed 450 nm laser excitation of coumarin-343 adsorbed on colloidal titanium dioxide. The TiO₂ sol (2.0 g/ℓ) in 5:1 (v/v) ethanol-methanol solvent mixture was containing 1.3×10^{-5} M of the coumarin dye. pH was adjusted to 3.5 by addition of HCl. Inserts show typical oscillograms recorded at the wavelengths $\lambda = 380$, 440 nm and 650 nm. Full time scale is in each case equal to 2 μs.
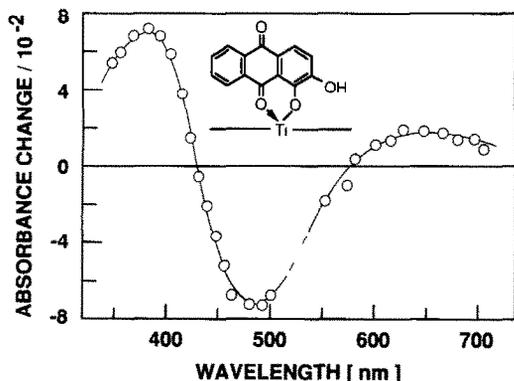

Fig. 2. Transient absorption spectrum observed 250 ns after pulsed 530 nm laser excitation of alcoholic colloidal titanium dioxide (0.5 g/ℓ) surface derivatized by alizarin 5×10^{-5} M. pH 3.5.

tained by laser photolysis of dye coated TiO₂ nanocrystals dispersed in the ethanol/ methanol 5:1 (v/v) solvent mixture at 23°C. The solvent was acidified by addition of 3.2×10^{-4} M HCl to prevent precipitation of the colloid. Detailed experimental conditions are indicated in the figure legends. The end of pulse spectra exhibit a bleaching in the vicinity of the absorption maxima of the sensitizers. The transient absorption peaks below 500 nm and above 600 nm
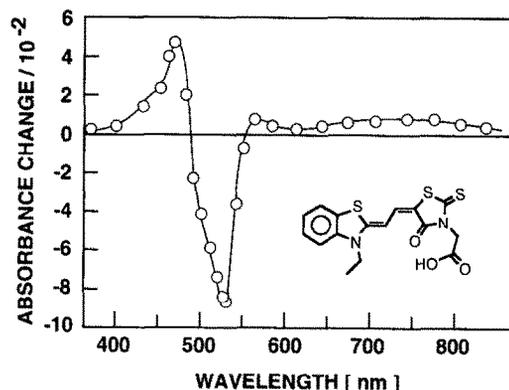

Fig. 3. Transient absorption spectrum observed 200 ns after pulsed 530 nm laser excitation of the merocyanine Mc2 adsorbed on colloidal TiO₂. The titanium dioxide sol (1.0 g/ℓ) in 5:1 (v/v) ethanol–methanol solvent mixture at pH 3.5 was containing 2×10^{-5} M of the merocyanine. In such conditions, no dye aggregate is formed on the oxide surface.

arise from the cation radicals of the dye and the conduction band electrons, respectively. Inserted in fig. 1 are oscilloscope traces showing the temporal behavior of the absorption at three different wavelengths. The vertical rise in the 380 and 650 nm absorption is due to the formation of coumarin-343 cation radicals and conduction band electrons, respectively, while the concomitant decrease in the absorption at 440 nm indicates the bleaching of the ground state. These optical changes are due to photoinduced electron injection from the dye into the conduction band of titanium dioxide:

$$S + h\nu \rightarrow S^* \rightarrow S^+ + e_{cb}^-(TiO_2) , \qquad (3)$$
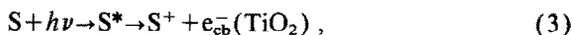
where S* and S⁺ are the excited state and the cation radical of the sensitizer, respectively. For all the three dyes tested here the injection is so rapid that it occurs during the laser pulse. The decline in the transient absorption and bleaching signals as shown as an example in fig. 1 is due to the thermal back reaction involving recapture of the conduction band electron by the dye cation radical.
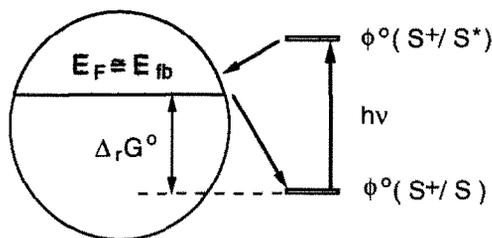
$$S^+ + e_{cb}^-(TiO_2) \rightarrow S . \qquad (4)$$

This process follows first order kinetics. The rate constant derived from the three oscillograms being practically identical. This confirms that eq. (4) represents the only redox process that follows sensitized

charge injection.

Scheme 2 gives a pictorial representation of the energy levels involved in the interfacial electron transfer process. The equation employed to derive the free energy change, $\Delta_r G^0$ for the electron transfer (eq. (4)) is also indicated along with an example of the calculation. The driving force for the reverse electron transfer corresponds to the difference between the quasi Fermi level of the conduction band electron in the TiO$_2$ nanocrystals, E_F^*, and the standard redox potential of the sensitizer. The former is approximately equal to the equilibrium Fermi level E_F and flat band potential E_{fb}, due to n-doping of the particles by oxygen vacancies. The flat band potential of TiO$_2$ in alcohol was determined using a previously published procedure [8,11] adapted to involve conduction band electron transfer to 1-methyl-1'-tetradecyl-4,4'-bipyridinium (C$_{14}$MV^{2+}) upon bandgap irradiation of the colloidal semiconductor. At pH 3.5 the E_{fb} value in ethanol is -0.45 V against NHE.

Fig. 4 shows the effect of temperature on the rate constants for back electron transfer. For coumarin-343 there is practically no rate variation between 300 and 100 K. Similarly, for the merocyanine the temperature effect is very small. The rate constant decreases by less than a factor of two in the investigated range. The largest temperature effect is observed for alizarin. However, even in this case the decrease in
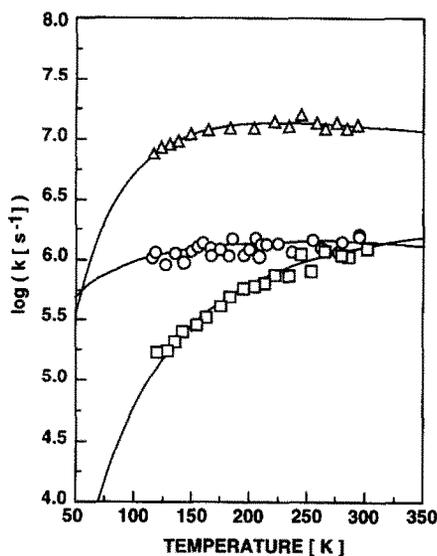

Fig. 4. Temperature dependence of the rate constant k for back electron transfer from colloidal TiO$_2$ conduction band to the radical cation of adsorbed alizarin ($\square$), merocyanine Mc2 ($\triangle$) and coumarin-343 ($\bigcirc$). Solid lines represent in each case the calculated optimal computer fit of eq. (9) to the experimental points. $\Delta_r G^0$ value was set to 1.65, -1.35 and -1.65 eV for the three sensitizers respectively. $\nu = 1500$ cm^{-1} was assumed for the vibrational mode frequency. Variation of the reorganization energy λ_s according to temperature dependence shown in table 2 was taken into account in the fitting procedure.

the rate constant is small, amounting to less than a factor of 10 over the 200 degrees temperature change.

4. Discussion

The results are interpreted in terms of current electron transfer theory. For a non-adiabatic process the rate constant is generally expressed in terms of the electronic matrix coupling element $|V|$ and the Franck–Condon factor FC [12]:

$$k = (2\pi/h) |V|^2 \, \text{FC} . \qquad (5)$$

Within the classical limit where the energy of the vibrational modes associated with the activated complex formation is smaller than the thermal energy ($h\nu \ll k_B T$):

$$\text{FC} = \sqrt{2\pi \lambda k_B T} \exp(-\Delta G^\dagger / k_B T) \qquad (6)$$

$$\Delta_r G^0 = -z\,F\,[\,\phi^0(\,S^+/\,S\,) - E_{fb}\,]$$

$$E_{fb}(TiO_2) = -0.260 - 0.059\,\text{pH} \;\;(\,V\,/\,NHE\,)$$

$$\text{pH} = 3.5 \;\;\rightarrow\;\; E_{fb}(TiO_2) = -0.450\,V$$

$$\phi^0(\,S^+/\,S\,) = 1.20\,V \;\;\rightarrow\;\; \Delta_r G^0 = -1.65\,\text{eV}$$

Scheme 2

and

$$\Delta G^{\dagger} = (\Delta_r G^0 + \Lambda)^2 / 4\Lambda , \qquad (7)$$

where $\Delta G^{\dagger}$ is the reaction activation energy. This gives eq. (2) for the rate constant of interfacial electron transfer. However the classical expression is not adequate to describe the results observed in fig. 4. Introducing the quantum modification for the Franck–Condon factor by assuming a single average high frequency mode yields [4]

$$FC = \sqrt{2\pi\lambda_s k_B T} \, \exp(-S_c)$$
$$\times \sum_{w=0}^{\infty} \frac{(S_c)^w}{w!} \exp\left(\frac{-(\Delta_r G^0 + wh\nu + \lambda_s)^2}{4\lambda_s k_B T}\right) . \qquad (8)$$

For the rate constant one obtains

$$k = \sqrt{\frac{\pi}{h^2 \lambda_s k_B T}} |V|^2 \sum_{w=0}^{\infty} \frac{\exp(-S_c)S_c^w}{w!}$$
$$\times \exp\left(\frac{-(\Delta_r G^0 + wh\nu + \lambda_s)^2}{4\lambda_s k_B T}\right) , \qquad (9)$$

where

$$S_c = \lambda_\nu / h\nu$$

is the Franck–Condon displacement factor, λ_ν and λ_s are the internal and solvent reorganization energies, respectively, and ν is the frequency of the vibrational mode associated with the electron transfer.

Eq. (9) was used to interpret the data. Solid lines of fig. 4 present the calculated optimal computer fit obtained by application of a modified Marquardt non-linear least-squares fitting procedure [13]. An average value of $\nu = 1500$ cm^{-1} was assumed in all cases for the vibrational mode frequency. Such a number was substantiated by resonance Raman experiments performed on alizarin/ colloidal TiO$_2$ systems, where the most active vibrational mode was measured at $\nu = 1450$ cm^{-1}. The parameters derived from the curve fitting are listed in table 1. The electronic matrix coupling element squared is 3 times larger for alizarin than for the coumarin. This can be rationalized from a consideration of the dye adsorption geometry shown in fig. 5. The configurations presented were optimized by using Tektronix CAChe molecular mechanics program package. The distances given indicate the separation of the center of the π-electron cloud of the sensitizer molecule from

Table 1
Free energies of reaction and fitted parameters of eq. (9), associated to the back electron transfer from TiO$_2$ conduction band to adsorbed sensitizers' radical cations. $\nu = 1500$ cm^{-1} was used in all cases as an average vibrational mode frequency in the fitting of experimental data. Values for λ_s, which is the only temperature dependent parameter, are given for $T = 298$ K

Sensitizer	$-\Delta G^0$ (eV)	$|V|^2$ (cm^{-1})	λ_ν (eV)	λ_s^{298} (eV)
alizarin–Ti^{IV}	1.65	5.6	0.32	0.004
merocyanine Mc2	1.35	4.1	0.28	0.08
coumarin-343	1.65	1.7	0.30	0.25

the plane of titanium atoms located at the oxide surface. The distance is 0.3 nm for alizarin, 0.4 nm for the merocyanine and 0.5 nm for coumarin-343. The decline in the value for electronic matrix coupling elements observed for the three sensitizers clearly reflects the decreasing overlap between the 3d wave function manifold of the surface titanium ions and the highest occupied molecular orbital of the sensitizer. Absolute values of the electronic coupling matrix elements $|V|^2$ are very low compared to homogeneous systems, where donor and acceptor molecules are separated by comparable distances. This fact arises from the delocalization of electrons in the semiconductor conduction band, as well as from orthogonality of adsorbed dye molecules with respect to the solid surface. The weak electronic coupling observed in these conditions ($|V|^2 < 10^{-3}$ eV) justifies here the application of a model which is restricted to the non-adiabatic electron transfer case ($|V|^2 < k_B T \approx 0.025$ eV).

The effect of temperature on the interfacial solvent reorganization energy was taken into account in the calculations. According to the Marcus equation for heterogeneous electron transfer, λ_s depends on the diameter of the dye molecule (d), the mean electron transfer distance, i.e. the separation of the molecule from the surface (r), the static dielectric constant of the solvent (ϵ), and the high frequency dielectric constant which is given by its refractive index squared (n^2):

$$\lambda_s = \frac{1}{2} \frac{(\Delta e)^2}{4\pi\epsilon_0} \left(\frac{2}{d} - \frac{1}{2r}\right)\left(\frac{1}{n^2} - \frac{1}{\epsilon}\right) . \qquad (10)$$
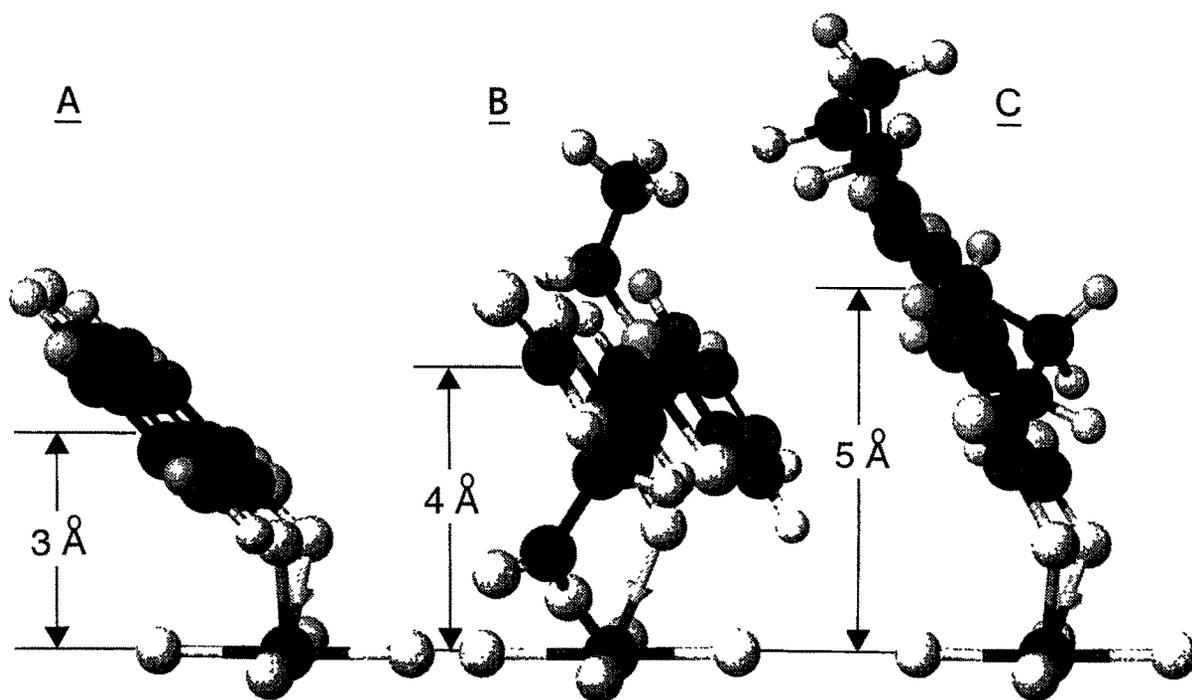
Fig. 5. Ball and stick three-dimensional molecular models for the attachment of alizarin (A), merocyanine Mc2 (B), and coumarin-343 (C) onto the titanium dioxide surface. Geometries were optimized using CAChe molecular mechanics program package. In each case, the distance separating the center of the π-electron cloud of the adsorbed sensitizer molecule from the plane of Ti atoms located at the TiO$_2$ surface is indicated.

The temperature increment of the static dielectric constant as well as that of the refractive index of ethanol is listed in table 2. From this analysis the variation of λ_s over the investigated temperature range of 200 K is about 2%.

While the internal reorganization energies derived from the computer fit of the data points in fig. 4 are close to 0.3 eV for all three sensitizers, the interfacial

Table 2
Temperature dependence of static and high frequency relative dielectric constant of ethanol and of solvent reorganization energy $\lambda_s \propto (1/n^2 - 1/\epsilon)$. Temperature coefficients $\alpha = -\text{d} \log \epsilon/\text{d}T \approx 2.9 \times 10^{-3} \text{ K}^{-1}$ and $\beta = -\text{d} \log n^2/\text{d}T \approx 2.0 \times 10^{-4} \text{ K}^{-1}$ could be considered as constant throughout the whole temperature domain $25°C > T > -120°C$ [14]

T (°C)	ϵ	n^2	$1/n^2 - 1/\epsilon$
25	24.3	1.8526	0.499
−60	41.0	1.9266	0.495
−120	61.8	1.9805	0.489

solvent reorganization energies vary greatly from one sensitizer to the other. The coumarin yields the highest value $\lambda_s^{298} = 0.25$ eV, and this is followed by the merocyanine for which $\lambda_s^{298} = 0.08$ eV. For the alizarin–Ti(IV) chelate, λ_s^{298} is close to zero. Using the electron transfer distances indicated in fig. 5 and for the van der Waals molecular diameters values of alizarin, merocyanine Mc2 and coumarin-343 1.2, 1.4 and 1.5 nm, one obtains from eq. (10) the interfacial solvent reorganization energies of 0, 0.10 and 0.21 eV, respectively. This is in satisfactory agreement with the values derived from the data in fig. 4.

For the alizarin–TiO$_2$ chelate, solvent reorganization appears to play a negligible role in the interfacial electron transfer process. This is supported by the finding that the rate of conduction band electron recapture by the alizarin radical cation is insensitive to the medium where the charge transfer is taking place. Preliminary experiments carried out with alizarin derivatized nanocrystalline TiO$_2$ films indicate that
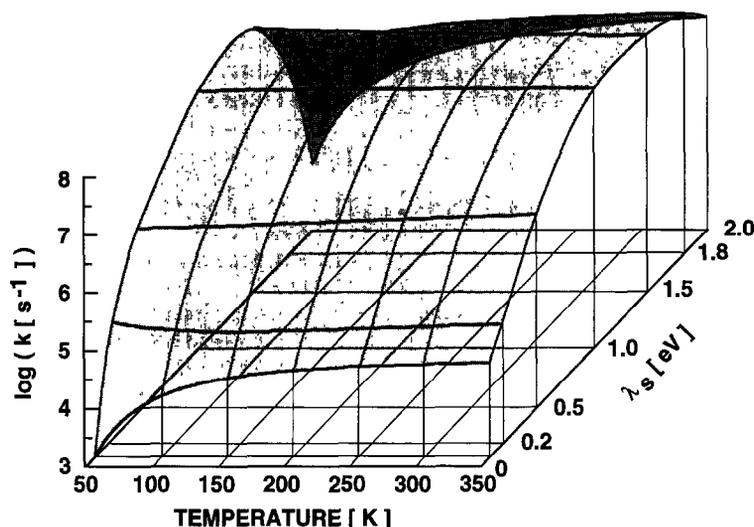
Fig. 6. Computer simulations of the temperature dependence of the electron transfer rate constant k according to eq. (9). Fixed parameters set in the equation were $\Delta_r G^0 = -1.5$ eV, $|V|^2 = 0.5$ cm^{-1}, $\nu = 1500$ cm^{-1} and $\lambda_v = 0.25$ eV. Values of the solvent reorganization energy λ_s^{298} were varied from 2.0 down to 0.1 eV. The dashed isotherm curves display the dependence of the rate constant versus λ_s at various temperature values. They represent distorted Marcus parabolas as the result of the quantum treatment of one single high frequency vibrational mode.

the rate observed in dry argon gas is similar to that in alcoholic solution. The rational for this unusual behavior is likely to be found in the very strong chelating interaction between the alizarin and the surface. This manifests itself by the fact that the oxidation potential and the absorption spectrum of the dye is profoundly affected by the binding to the TiO$_2$ surface, although they are practically insensitive to the polarity of the medium. Redox reactions involving the conduction band of the semiconductor and such types of chelates are therefore apparently not greatly affected by solvation.

In order to facilitate the understanding of the temperature effects on the interfacial electron transfer rates observed in the present study, we have plotted in fig. 6 a simulation of eq. (9) for various solvent reorganization energies, the other parameters being kept constant at the values indicated in the figure legend. In the normal Marcus regime, $\lambda_s + \lambda_v = \Lambda > -\Delta_r G^0$, a pronounced temperature effect on the rate constant is evident. An activationless behavior is attained when $\lambda_s + \lambda_v = -\Delta_r G^0$ and this persists in the inverted Marcus region where $\lambda_s + \lambda_v < -\Delta_r G^0$. Only for very small values of λ_s, where quantum effects be-

come dominant, is the temperature dependence restored.

References

[1] A.A.K. Vervast, W.P. Gomes and F. Cardon, J. Electroanal. Chem. Interface Electrochem. 91 (1978) 133;
J. Vandermolen, W.P. Gomes and F. Cardon, J. Electrochem. Soc. 127 (1980) 324;
M. Nishida, J. Appl. Phys. 51 (1980) 1669;
M.A. Butler, M. Abramovicz, F. Decker and J.F. Julino, J. Electrochem. Soc. 128 (1981) 200;
R. Memming, Electrochim. Acta 25 (1980) 77;

F.R.F. Fan and A.J. Bard, J. Am. Chem. Soc. 102 (1980) 3677;

H.K. Hovel, Solar cells, semiconductors and semimetals, Vol. 11 (Academic Press, New York, 1975) pp. 8–37;

H. Gerischer, Surface Sci. 101 (1980) 518;

M.A. Fox and M. Chanon, Photoinduced electron transfer (Elsevier, Amsterdam, 1988).

[2] J.O'M. Bockris and A.K.N. Reddy, Modern electrochemistry, Vol. 2 (Plenum Press, New York, 1973).

[3] R.A. Marcus and N. Sutin, Biochim. Biophys. Acta 811 (1985) 265.

[4] J.R. Miller, J.V. Beitz and R.K. Huddleston, J. Am. Chem. Soc. 106 (1984) 5057;

G.L. Closs, L.T. Calcaterra, J. Green, K.W. Penfield and J.R. Miller, J. Am. Chem. Soc. 90 (1986) 3673;

I.R. Gould, D. Ege, J.E. Moser and S. Farid, J. Am. Chem. Soc. 112 (1990) 4290.

[5] N. Liang, J.R. Miller and G.L. Closs, J. Am. Chem. Soc. 111 (1989) 8740; 112 (1990) 5353.

[6] M. Bixon and J. Jortner, J. Phys. Chem. 95 (1991) 1941.

[7] J. Moser and M. Grätzel, Helv. Chim. Acta 65 (1982) 1436.

[8] D. Duonghong, J. Ramsden and M. Grätzel, J. Am. Chem. Soc. 104 (1982) 2977.

[9] B. O'Regan, J. Moser, M. Anderson and M. Grätzel, J. Phys. Chem. 94 (1990) 8720.

[10] M.K. Nazeeruddin, P. Liska, J. Moser, N. Vlachopoulos and M. Grätzel, Helv. Chim. Acta 73 (1990) 1788.

[11] J. Moser and M. Grätzel, J. Am. Chem. Soc. 105 (1983) 6547.

[12] R.A. Marcus, J. Chem. Phys. 24 (1956) 966.

[13] D.W. Marquardt, Chem. Eng. Progr. 55 (1959) 65; J. Soc. Ind. Appl. Math 11 (1963) 431;

C. Daniel and F.S. Wood, Fitting equations to data (Wiley, New York, 198.

[14] R.C. Weast, ed., CRC handbook of chemistry and physics, 57th Ed. (CRC Press, Cleveland, 1976).